


## ORIGINAL ARTICLE

# Bacterial phototoxicity of biomimetic CdTe-GSH quantum dots

N. Oetiker<sup>1</sup>, C. Muñoz-Villagrán<sup>2</sup>, C.C. Vásquez<sup>2</sup>, D. Bravo<sup>3</sup> and J.M. Pérez-Donoso<sup>1</sup> 

<sup>1</sup> BioNanotechnology and Microbiology Laboratory, Center of Bioinformatics and Integrative Biology (CBIB), Biological Sciences Faculty, Universidad Andres Bello, Santiago, Chile

<sup>2</sup> Molecular Microbiology Laboratory, Chemistry and Biology Faculty, Universidad de Santiago de Chile, Santiago, Chile

<sup>3</sup> Oral Microbiology Laboratory, Dentistry Faculty, Universidad de Chile, Santiago, Chile

## Keywords

biomimetic quantum dots, CdTe-GSH, photodynamic therapy, phototoxicity.

## Correspondence

José M. Pérez-Donoso, BioNanotechnology and Microbiology Laboratory, Center of Bioinformatics and Integrative Biology (CBIB), Biological Sciences Faculty, Universidad Andres Bello, Santiago, Chile.  
E-mail: jose.perez@unab.cl

2020/1633: received 4 August 2020, revised 12 November 2020 and accepted 29 November 2020

doi:10.1111/jam.14957

## Abstract

**Aim:** Fluorescent semiconductor nanoparticles or quantum dots (QDs) have excellent properties as photosensitizers in photodynamic therapy. This is mainly a consequence of their nanometric size and the generation of light-activated redox species. In previous works, we have reported the low-cost biomimetic synthesis of glutathione (GSH) capped QDs (CdTe-GSH QDs) with high biocompatibility. However, no studies have been performed to determine their phototoxic effect. The aim of this work was to characterize the light-induced toxicity of green (QDs<sub>500</sub>) and red (QDs<sub>600</sub>) QDs in *Escherichia coli*, and to study the molecular mechanism involved.

**Methods and Results:** Photodegradation and reduction power of biomimetic QDs was determined to analyse their potential for radical generation. *Escherichia coli* cells were exposed to photoactivated QDs and viability was evaluated at different times. High toxicity was determined in *E. coli* cells exposed to photoactivated QDs, particularly QDs<sub>500</sub>. The molecular mechanism involved in QDs phototoxicity was studied by determining Cd<sup>2+</sup>-release and intracellular reactive oxygen species (ROS). Cells exposed to photoactivated QDs<sub>500</sub> presented high levels of ROS. Cells exposed to photoactivated QDs<sub>500</sub> presented high levels of ROS. Finally, to understand this phenomenon and the importance of oxidative and cadmium-stress in QDs-mediated phototoxicity, experiments were performed in *E. coli* mutants in ROS and Cd<sup>2+</sup> response genes. As expected, *E. coli* mutants in ROS response genes were more sensitive than the wt strain to photoactivated QDs, with a higher effect in green-QDs<sub>500</sub>. No increase in phototoxicity was observed in cadmium-related mutants.

**Conclusion:** Obtained results indicate that light exposure increases the toxicity of biomimetic QDs on *E. coli* cells. The mechanism of bacterial phototoxicity of biomimetic CdTe-GSH QDs is mostly associated with ROS generation.

**Significance and Impact of the Study:** The results presented establish biomimetic CdTe-GSH QDs as a promising cost-effective alternative against microbial infections, particularly QDs<sub>500</sub>.

## INTRODUCTION

The persistent increase in infections associated with multidrug-resistant pathogens has favoured the interest in developing new antimicrobial alternatives capable of efficiently eliminate pathogenic micro-organisms and, at the same

time, avoid the generation of antibiotic resistance (Cieplik *et al.* 2018). Currently, near 700 000 deaths are attributed to antibiotic resistance, and it is projected that by 2050 there will be more than 10 million cases (Renwick *et al.* 2016).

Photodynamic therapy (PDT) is an innovative clinical treatment based on the activation of light-absorbing

molecules or photosensitizers (PSs), which after irradiation at a specific wavelength, generate reactive oxygen species (ROS). The PSs are initially in a singlet state (basal state of energy  $S_0$ ) and after the absorption of photons changes to an excited state ( $S_1$ ) (Nishiyama *et al.* 2009). This excited state is unstable, so the PSs return to their ground state through fluorescence emission or moves to the excited triplet state ( $T_1$ ), which is more stable than  $S_1$ . Then, the PSs in  $T_1$  can transfer hydrogen, electrons or direct energy to the surrounding oxygen, thus generating ROS (Celli *et al.* 2010; Yi *et al.*, 2018; Ye, Yan *et al.*, 2020; Ye, Zeng *et al.*, 2020). These therapies are currently applied for the treatment of some superficial cancers and infections caused by bacteria and fungi (Wolf *et al.* 1993; Michailov *et al.* 1997; Souza *et al.* 2010; Koshi *et al.* 2011; de Oliveira *et al.* 2014; Cieplik *et al.* 2018). The use of this kind of sensitizers for the treatment of infections is called antimicrobial photodynamic therapy (aPDT).

In this context, there is considerable interest in improving the effect of PDT and aPDT by developing new PSs with low toxicity in the absence of light, high photostability, high capacity to produce ROS, and involving simple, economic and sustainable synthesis processes. Currently, there are many reports of clinical applications of aPDT for the treatment of infections produced by different micro-organisms (Lombard and Lanotte 1985; Abramson *et al.* 1992; Shikowitz *et al.* 1998; Asilian and Davami 2006; Christodoulides *et al.* 2008; Brown *et al.* 2009; Kharkwal *et al.* 2011; da Mota *et al.* 2015).

Semiconductor nanoparticles (NPs) or quantum dots (QDs) are composed of elements like cadmium (Cd), sulphur (S), selenium (Se) or tellurium (Te) that given their particular physicochemical and optoelectronic properties exhibit great technological potential (Monrás *et al.* 2012). QDs have a core size between 1 and 20 nm (Chen *et al.* 2012; Díaz *et al.* 2012; Pérez-Donoso *et al.* 2012) and their size of QDs determines their spectroscopic properties, displaying fluorescence emissions varying from 450 nm (blue-green) to 650 nm (red) (Zheng *et al.* 2007; Rosenblum *et al.* 2010; Chen *et al.* 2012; Pérez-Donoso *et al.* 2012). QDs have broad absorption spectra, narrow fluorescence peaks, and are photostable (Zheng *et al.* 2007; Smith *et al.* 2008; Rosenblum *et al.* 2010; Chen *et al.* 2012). Also, the fluorescence sensibility of QDs is two to three times higher than most organic fluorophores commonly used in live imaging (Díaz-García *et al.* 2018), a situation that has favoured their use as a fluorescent tool for *in vivo* assays. The surfaces of QDs can be modified, improving their active targeting, or the addition of diagnostic or therapeutic groups (Akerman *et al.* 2002; Zheng *et al.* 2007; Smith *et al.* 2008; Delehanty *et al.* 2009). QDs capped with thiols are more soluble and could be

prepared directly from the aqueous solution because thiols act as stabilizers (Gaponik *et al.* 2002; Zheng *et al.* 2007). Some studies have shown that the *in vitro* cellular toxicity of cadmium-based QDs depends on their capability of releasing  $Cd^{2+}$  ions and also on the nature of the organic capping that protects the QDs from oxidation and determines their cellular distribution (Lewinski *et al.* 2008; Pons *et al.* 2010).

QDs have been applied in PDT, and it has been determined that photoexcited CdTe QDs (2.4 eV) can inhibit the growth of many clinically relevant bacterial pathogens highly resistant to drugs (Courtney *et al.* 2016). This lethal effect is related to selective alteration of the redox state of QDs, a result that confirms their role as PSs.

Most QDs synthesis methods described to date involve the use of organic solvents, high temperatures and anaerobic environments. Under these conditions, QDs synthesized display high production costs, hydrophobicity and high levels of toxicity in biological systems (Li *et al.* 2009; Wang *et al.* 2009; Iravani *et al.* 2016). In this context, several protocols for the aqueous synthesis of soluble NPs have been described (Qu and Lü 2009; Song *et al.* 2012); however, most of them generate NPs with low biocompatibility (Henderson and Dougherty 1992; You *et al.* 2013), thus affecting their application in biological systems.

In 2012 we reported a simple, low cost and biomimetic protocol to synthesize red and green-emitting QDs. The method requires  $CdCl_2$ ,  $K_2TeO_3$  and glutathione (GSH) as a capping and reducing agent. Highly fluorescent CdTe-GSH QDs are obtained at temperatures, pH values and oxygen conditions similar to those found in microbial cells (biomimetic) (Pérez-Donoso *et al.* 2012) (patent n° US 20130284979). GSH is a thiol-containing oligopeptide found in most organisms, and it plays an important role in the detoxification of heavy metals in cells. The physiological mechanism of detoxification involves the binding of heavy-metal nanoclusters by GSH (Grill *et al.* 1985; Schafer and Buettner 2001). GSH is also involved in chromate, Zn (II), Cd(II) and Cu(II) homeostasis and resistance in *Escherichia coli* (Helbig *et al.* 2008). Taking into consideration the redox properties of GSH, its abundance in cells (eukaryotes and Gram-negative bacteria principally) and the previously described stabilization of CdSe and CdTe QDs by this tripeptide (Zheng *et al.* 2007), we decided to use this biological thiol as a reducing and capping agent for the aqueous synthesis of CdTe QDs.

Biomimetic QDs present high biocompatibility to eukaryotic cells (Pérez-Donoso *et al.* 2012), does not produce DNA fragmentation or changes in cell morphology (Díaz *et al.* 2012), and generate low levels of cell death associated with necrosis (Pérez-Donoso *et al.* 2012;

Gautier *et al.* 2013). Nevertheless, biomimetic QDs slightly affect the growth of *E. coli*, *Bacillus subtilis*, *Klebsiella pneumoniae* and *Staphylococcus aureus* at concentrations as high as  $500 \mu\text{g ml}^{-1}$  (Díaz *et al.* 2012). Furthermore, microarrays analysis revealed changes in DNA expression in *E. coli* cultures after exposure to CdTe-GSH QDs, determining that bacterial toxicity of biomimetic QDs was mainly related to the release of  $\text{Cd}^{2+}$  ions, the production of oxidative stress and loss of membrane integrity (Monrás *et al.* 2014). Increased toxicity was determined in red QDs, a result associated with the increased Cd-content and metal release from the core of these NPs. *Escherichia coli* MICs for green and red biomimetic CdTe-GSH QDs are 2000 and  $125 \mu\text{g ml}^{-1}$ , respectively, confirming that these QDs display differential toxicity, being red QDs clearly more toxic than green NPs (Monrás *et al.* 2014). Also, thiol capped QDs present increased solubility and lower toxicity than QDs produced by other chemical methods (Helbig *et al.* 2008; Perez-Donoso *et al.* 2012).

More recently, the effect of biomimetic QDs *in vivo* systems was evaluated. Our red and green biomimetic fluorescent NPs were used to track metastatic cells in mice with no effect on animal viability (Díaz-García *et al.* 2018). QDs-labelled B16F10 cells remained viable for at least 5 days and migrated similarly to control cells. However, the capacity to form metastatic nodules in the lungs was attenuated. Fluorescence imaging showed that QDs-labelled B16F10 cells can be tracked following injection into C57BL/6 mice, and these cells preferentially accumulated in the perialveolar area of the lungs (Díaz-García *et al.* 2018). Despite all these antecedents regarding the effect of biomimetic CdTe-GSH QDs in different biological systems, no studies to determine their phototoxic effect have been performed to date.

In the present work, we studied the mechanism of bacterial phototoxicity of green- and red-emitting biomimetic QDs (emission  $\lambda = 500$  and  $600$  nm). To understand the importance of oxidative and cadmium-stress in QDs-mediated phototoxicity, experiments were performed in *E. coli* mutants in ROS and  $\text{Cd}^{2+}$  response genes. Altogether obtained results allowed us to characterize the properties of biomimetic QDs and their potential as new PSs for aPDT.

## MATERIALS AND METHODS

### Synthesis of CdTe GSH QDs

QDs were synthesized by using a protocol previously described by our group (Pérez-Donoso *et al.* 2012, patent no. US 20130284979). A synthesis solution containing  $\text{CdCl}_2$   $40 \mu\text{mol l}^{-1}$ ,  $\text{K}_2\text{TeO}_3$   $10 \mu\text{mol l}^{-1}$  and GSH

$10 \text{ mmol l}^{-1}$  was prepared in citrate/ $\text{NaBH}_4$   $15 \text{ mmol l}^{-1}$  (pH = 9.4) buffer. The solution was incubated at  $90^\circ\text{C}$  for 2 h (QDs<sub>500</sub>) or 6 h (red QDs<sub>600</sub>) and the reaction was stopped by cooling ( $4^\circ\text{C}$ ). QDs were dialysed in citrate/ $\text{NaBH}_4$   $15 \text{ mmol l}^{-1}$  at pH 9.4 during 2 h. Afterwards, QDs were precipitated using 2 volumes of ethanol for 10 min at  $-20^\circ\text{C}$ . Solutions were then centrifuged at  $24\,000 \text{ g}$  at  $4^\circ\text{C}$  for 20 min. Pellets were purified and vacuum dried 24 h at room temperature. Finally, QDs were dissolved in nanopure water as described previously (Pérez-Donoso *et al.* 2012).

### Photobleaching of QDs<sub>500</sub> and QDs<sub>600</sub>

The photostability of QDs was evaluated in liquid media. A  $400 \mu\text{g ml}^{-1}$  suspension of QDs was prepared and irradiated 1 h at 470 or 530 nm for QDs<sub>500</sub> or QDs<sub>600</sub> respectively. The fluorescence was evaluated at different time points and the decay in fluorescence was determined. Fluorescence was measured in microplates using a Sinergy H1M reader (Biotek).

### Phototoxicity assay

#### Viability Assay

*Escherichia coli* BW 25113 in exponential phase of growth was exposed to QDs<sub>500</sub> or QDs<sub>600</sub> ( $400 \mu\text{g ml}^{-1}$ ) in sterile buffer PBS  $50 \text{ mmol l}^{-1}$ , pH 7.5 and irradiated at 405 nm (5 mW) during different time intervals (0, 5, 10, 15, 20 and 30 min). Then, samples were serially diluted (1 : 10) in PBS and 10 ml of each dilution was seeded on LB plates to determine the number of colony-forming units (CFU). The number of CFU per ml was calculated using the formula:  $[(\# \text{colonies}) \times (\text{dilution factor})]/(\text{volume plated in ml})$  as described previously (Molina-Quiroz *et al.* 2014).

### Growth inhibition area

To assess growth inhibition zones of *E. coli* mutants in ROS and cadmium responsive genes, 0.5 ml of exponentially growing bacterial cultures (1/10 dilution) was evenly distributed on LB plates. Then,  $5 \mu\text{l}$  of a QDs solution ( $50 \text{ mg ml}^{-1}$ ) was deposited on the plate. To evaluate the effect of irradiation, the plates were exposed for 5 min to 405 nm light (5 mW). Plates were incubated 24 h at  $37^\circ\text{C}$  and growth inhibition zones were determined by measuring halos diameters as previously reported (Pérez *et al.* 2007; Díaz *et al.* 2012).

### Intracellular ROS generation

ROS generation was measured using the ROS-sensitive fluorescent probe  $\text{H}_2\text{DCFDA}$  dye. *Escherichia coli* grown

in exponential phase (OD: 0.3–0.4) was irradiated at 405 nm (5 mW) for 10, 15 and 20 min. Then, cells were incubated with H<sub>2</sub>DCFDA for 30 min, washed twice in cold PBS and analysed by flow cytometry. As positive control cells were exposed to H<sub>2</sub>O<sub>2</sub> (1 mmol l<sup>-1</sup>).

#### Release of cadmium ions from biomimetic QDs

QDs<sub>500</sub> and QDs<sub>600</sub> were resuspended in PBS buffer (1 mg ml<sup>-1</sup>) and the concentration of Cd ions in solution after 10 min exposure to 405 nm irradiation was determined by flame atomic absorption spectroscopy as described previously (Venegas *et al.* 2017). One hundred microlitre samples were diluted to 4 ml of milliQ water and measured in a FAAS equipment (Shimadzu). A Cd calibration curve was built using a commercial standard (Sigma Aldrich).

#### Bacterial strains and growth conditions

*Escherichia coli* BW25113 was the wild type (wt) strain used in all experiments. *Escherichia coli* deletion mutants were provided by the NARA Institute of Science and Technology, Japan (Baba *et al.* 2006). Cell cultures were routinely grown in LB medium at 37°C with constant shaking and the antibiotic kanamycin (50 µg ml<sup>-1</sup>) was added when required. Kan<sup>R</sup> insertions into *E. coli* BW25113 chromosomal genes were constructed by the method of Datsenko and Wanner (2000).

#### Statistical analyses

Statistical analyses were performed by *t*-student using GraphPad Prism 7 version 7.0a, a significance level of *P* < 0.05 was adopted for all analyses.

## RESULTS

#### Physical and photophysical properties

In previous reports, we characterized the chemical, spectroscopic and physical properties of biomimetic CdTe-GSH QDs, particularly green QDs and red QDs with fluorescence emissions at 500 and 600 nm respectively (Díaz *et al.* 2012; Gautier *et al.* 2013; Monrás *et al.* 2014; Díaz-García *et al.* 2018). Size, photostability and energy states of QDs are particularly relevant properties that can affect the production of ROS (Lovrić *et al.* 2005). Red QDs showed higher polydispersity and size than green QDs, with average hydrodynamic diameters of 11.33 and 1.86 nm respectively (Díaz *et al.* 2012; Gautier *et al.* 2013; Monrás *et al.* 2014; Díaz-García *et al.* 2018). Based on spectroscopic data, green QDs present a higher band

gap (24 679 eV at 470 nm) than red QDs (20 540 eV at 530 nm). This result reveals that green QDs have higher reduction power to form singlet oxygen, superoxide radicals and other ROS as compared to red QDs (Nozik 1978; Katari *et al.* 1994).

Photobleaching is a dynamic process initiated by the photocatalytic oxidation of the thiol ligands on the surface of the nanocrystals, generating photooxidation and precipitation of the NPs. The photooxidation occurs in the presence of singlet oxygen or other ROS present in the solution (Aldana *et al.* 2001; Ferreira *et al.* 2006, 2007). To estimate the potential production of singlet oxygen by biomimetic QDs, the photodegradation rate of aerated aqueous solutions after irradiation at 450 nm and 44 490 mW cm<sup>-2</sup> was measured (Fig. 1). Green QDs were photodegraded at a higher rate than red QDs, a result that suggests that QDs<sub>500</sub> produce higher levels of ROS and represents excellent candidates for PDT. During the 60 min irradiation of the experiment, no precipitation of nanocrystals was observed (data not shown), a situation that reflects moderate levels of oxidation since it has been reported that nanocrystals precipitation only occurs after severe oxidation (Aldana *et al.* 2001).

#### Phototoxicity of CdTe-GSH QDs

We studied the phototoxicity of green and red QDs biomimetic CdTe-GSH QDs on *E. coli* (Fig. 2). The cellular viability of *E. coli* cells exposed to 400 µg ml<sup>-1</sup> of green or red QDs (a non-toxic concentration as determined before, Díaz *et al.* 2012) without irradiation (Fig. 2a,b), or irradiated at 405 nm during 5, 10, 15, 20 or 30 min was determined (Fig. 2).

Under the experimental conditions tested, no effects on viability were observed on nonirradiated cells exposed to QDs (Fig. 2a,b). In the absence of QDs, *E. coli* cells irradiated at 405 nm (5 mW) show a significative decrease in viability after 15 min irradiation (Fig. 2c). When cells were exposed to irradiated green QDs, the viability of cells decreased significantly after 5-min irradiation with more than 50% of dead cells (Fig. 2d). In the case of cells exposed to irradiated red QDs, a decrease of approximately 40% on viable cells was observed after 5-min irradiation (Fig. 2e), with a higher decrease after 10 min (near 50% of dead cells). The observed increased toxicity of irradiated green QDs is an interesting result particularly considering that previous results indicate that, in the absence of irradiation, red QDs are much more toxic for bacterial cells (Díaz *et al.* 2012; Pérez-Donoso *et al.* 2012).

Altogether, viability results revealed the existence of a photodynamic effect on biomimetic CdTe-GSH QDs.

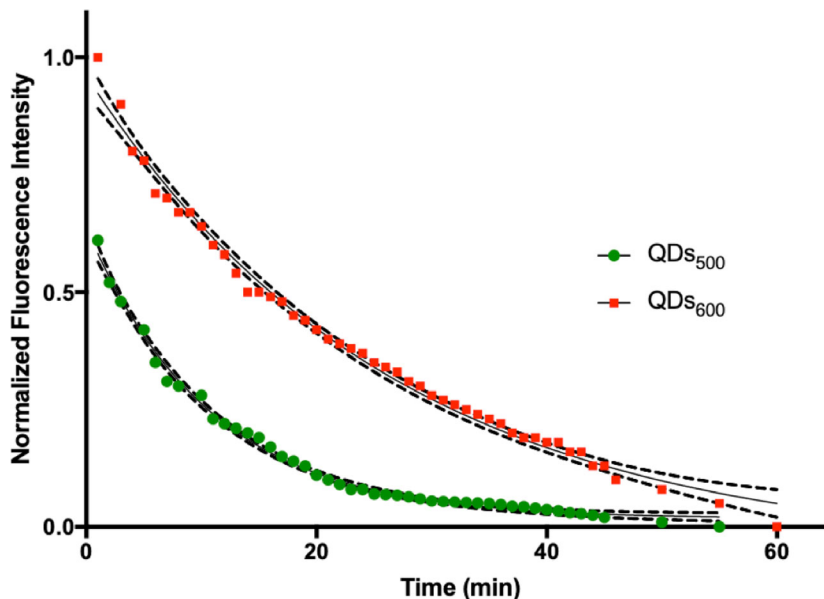


Figure 1 Photobleaching of QDs500 and QDs600. QDs500 and QDs600 are shown in green and red respectively.

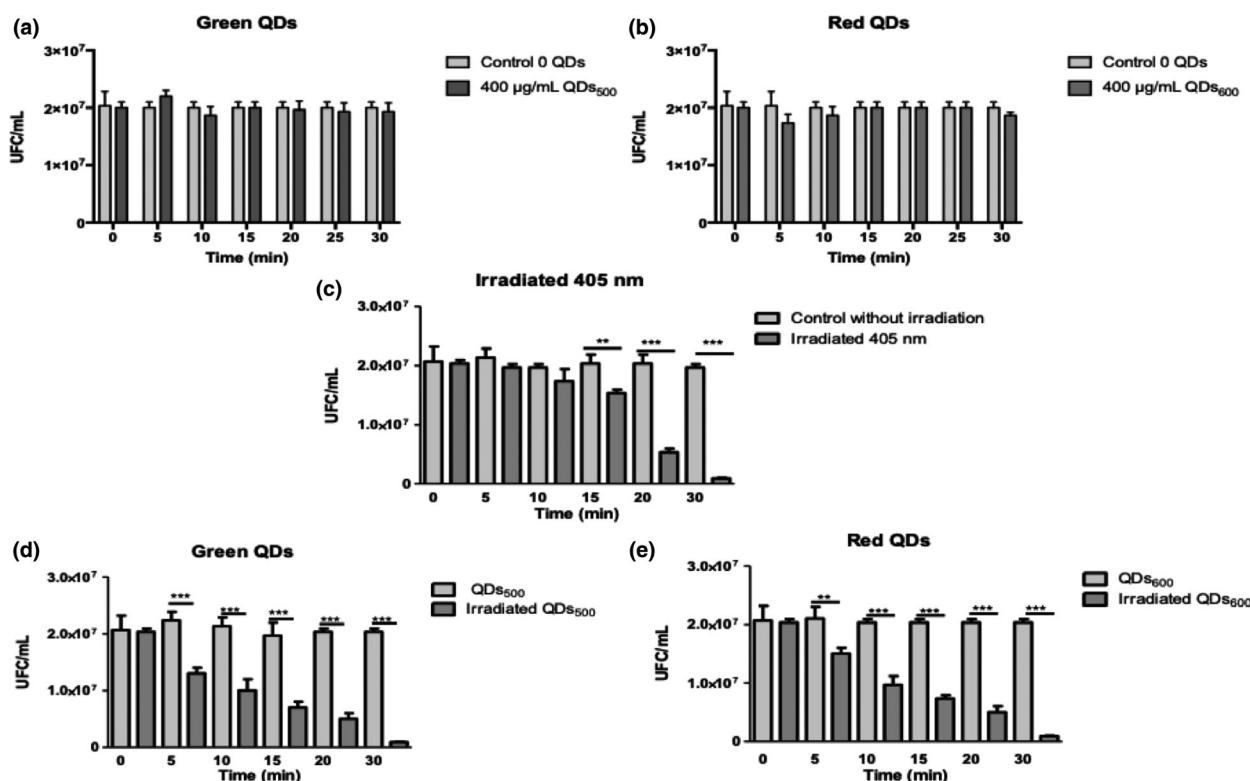
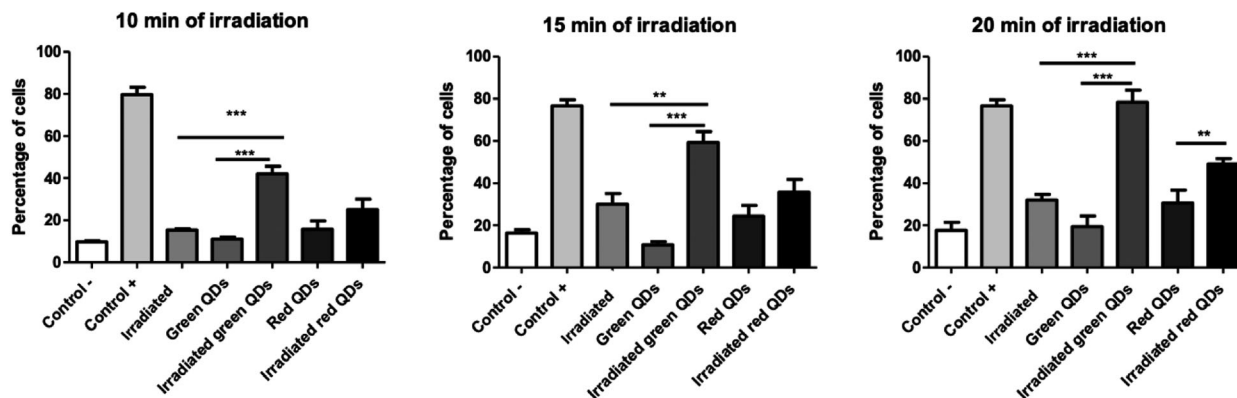


Figure 2 Phototoxic effect of QDs500 and QDs600 in *Escherichia coli*. Viability of *E. coli* exposed to (a) green QDs500 ( $400 \mu\text{g ml}^{-1}$ ), and (b) red QDs600 ( $400 \mu\text{g ml}^{-1}$ ) during 5, 10, 15, 20, and 30 min. Control correspond to cells non-exposed to QDs. (c) Viability of *E. coli* cells exposed to irradiation (405 nm) in absence of QDs. (d) Viability of *E. coli* cells exposed to QDs500 and irradiated (405 nm) during different times. (e) Viability of *E. coli* cells exposed to QDs600 and irradiated (405 nm) during different times. Statistical analysis *T*-test show  $***P \leq 0.001$ ,  $**P \leq 0.01$  and  $*P \leq 0.05$ .



**Figure 3** Intracellular ROS generation in *Escherichia coli* exposed to QDs500 and QDs600 after irradiation at 405 nm. ROS generation was measured using the ROS sensitive fluorescent probe H<sub>2</sub>DCFDA. *Escherichia coli* BW 25113 cells were irradiated at 405 nm during (a) 10, (b) 15 and (c) 20 min, and the fluorescence of cells was evaluated by flow cytometry. Control +: H<sub>2</sub>O<sub>2</sub>; Control -: cells in absence of QDs and irradiation. T-test was used for statistical analysis (\*\*\**P* ≤ 0.001, \*\**P* ≤ 0.01 and \**P* ≤ 0.05).

### Mechanism of biomimetic CdTe-GSH QDs phototoxicity in *E. coli*

In a previous work, we determined that part of biomimetic QDs toxicity in *E. coli* involved the generation of ROS (Monrás et al. 2014). In this context, we decided to evaluate the effect of irradiation on ROS generation in cells exposed to green and red biomimetic QDs. Intracellular ROS generation was measured using the ROS-sensitive fluorescent probe H<sub>2</sub>DCFDA. *Escherichia coli* BW25113 was irradiated at 405 nm (5 mW) during 10, 15 and 20 min in the presence or absence of QDs, and ROS generation was determined by flow cytometry (Fig. 3).

No increase in ROS levels was determined in *E. coli* cells exposed to green QDs (400 µg ml<sup>-1</sup>). Similar levels to those observed in cells nonexposed to QDs or irradiation were determined (Fig. 3a–c). This result is in agreement with the scarce effect observed in viability under this condition (Fig. 2a). However, when cells were

exposed to photoactivated green QDs<sub>500</sub>, ROS generation was observed after 5 min, reaching 80% of fluorescent cells after 20 min (similar to the positive control). In the case of red QDs<sub>600</sub>, a significant difference in ROS generation between irradiated and non-irradiated cells was only observed after 20-min exposure (Fig. 3c).

At this point, obtained results indicate that green QDs<sub>500</sub> display increased phototoxicity than red QDs<sub>600</sub> due to its higher reduction potential (Eg) that favours the production of ROS. However, this does not rule out the possibility that part of the observed phototoxicity of QDs<sub>500</sub> could be a consequence of the release of Cd<sup>2+</sup> ions from the QDs metal core (photodegradation). To test this possibility, the release of Cd<sup>2+</sup> ions by green QDs<sub>500</sub> and red QDs<sub>600</sub> was determined (Fig. 4).

As expected, the level of cadmium ions determined in non-irradiated green QDs<sub>500</sub> solutions was minor to that generated by red QDs<sub>600</sub> (Fig. 4). This is in agreement with previous results revealing the importance of Cd<sup>2+</sup> on the

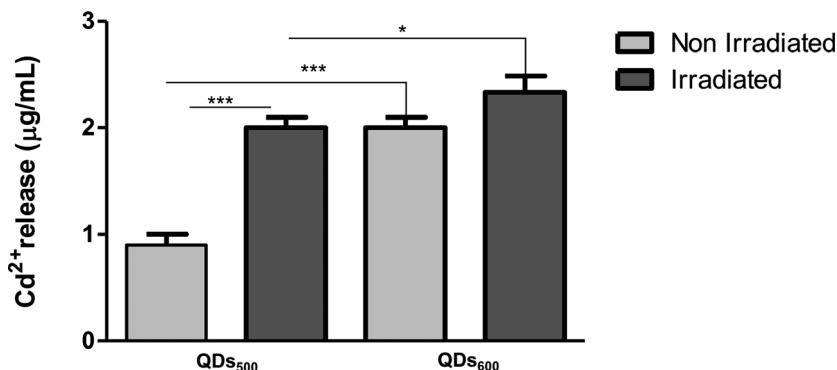


**Figure 4** Effect of irradiation on cadmium release from CdTe-GSH biomimetic QDs. T-test was used for statistical analysis (\*\*\**P* ≤ 0.001, \*\**P* ≤ 0.01 and \**P* ≤ 0.05).

increased toxicity determined by red QDs<sub>600</sub> in the absence of irradiation (Ochi *et al.* 1988; Derfus *et al.* 2004; Hardman 2006; Rzigalinski and Strobl 2009; Monrás *et al.* 2014). Regarding the effect of irradiation on Cd-release, no statistically significant differences were observed between irradiated and non-irradiated red QDs<sub>600</sub>. However, the irradiation of green QDs<sub>500</sub> strongly increases the amount of released cadmium. This result is consistent with photodegradation experiments in Fig. 1, indicating that green QDs<sub>500</sub> have a high photodegradation rate than red QDs<sub>600</sub>, and are also in agreement with the increased levels of ROS determined in green QDs. Altogether, obtained results suggest that QDs phototoxicity is mostly associated with ROS production and is not directly related to metal release. To understand this phenomenon, we decided to study the effect of irradiated QDs on *E. coli* mutants in ROS and Cd homeostasis genes.

#### Phototoxic effect of CdTe-GSH QDs on *E. coli* mutants in ROS-response genes

Considering the levels of ROS production determined in cells exposed to irradiated QDs, we decided to analyse the effect of irradiated QDs in *E. coli* strains deficient in ROS response genes (*hpx*, *sodA/sodB* or *kat*), to evaluate the contribution of oxidative stress to the phototoxicity of biomimetic QDs. All genes analysed encode

protective proteins that directly participate in ROS detoxification. The radical superoxide ( $O_2^{\bullet -}$ ) generated during ROS production is transformed into hydrogen peroxide ( $H_2O_2$ ) by a family of enzymes called superoxide dismutase (*sod*). On the other hand, the HPX genes (*hpx*) are involved in the decomposition of  $H_2O_2$ , and catalases (*kat*) catalyse the dismutation of hydrogen peroxide into water and oxygen (Molina-Quiroz *et al.* 2013; Dharmaraja 2017).

In the absence of irradiation, wt and mutant *E. coli* cells presented a similar sensitivity to green QDs, as determined by the growth inhibition area (Fig. 5). This result was expected considering the low levels of ROS produced by non-irradiated green QDs. In contrast, all mutants display increased sensitivity when were exposed to irradiated QDs<sub>500</sub> (Fig. 5a), a result that is in agreement with the increased levels of ROS determined in cells exposed to photoactivated QDs (Fig. 3). On the other hand, when wt,  $\Delta$ *sodA/sodB* and  $\Delta$ *kat* strains were exposed to red QDs<sub>600</sub>, no significant differences in cellular toxicity were observed between the wt and the mutant strains (Fig. 5b). In addition, no differences were determined between irradiated and non-irradiated cells (Fig. 5b), a result suggesting that the scarce phototoxicity observed under these conditions is not a consequence of ROS generation. In contrast,  $\Delta$ *hpx* cells exposed to red QDs<sub>600</sub> presented a significant growth

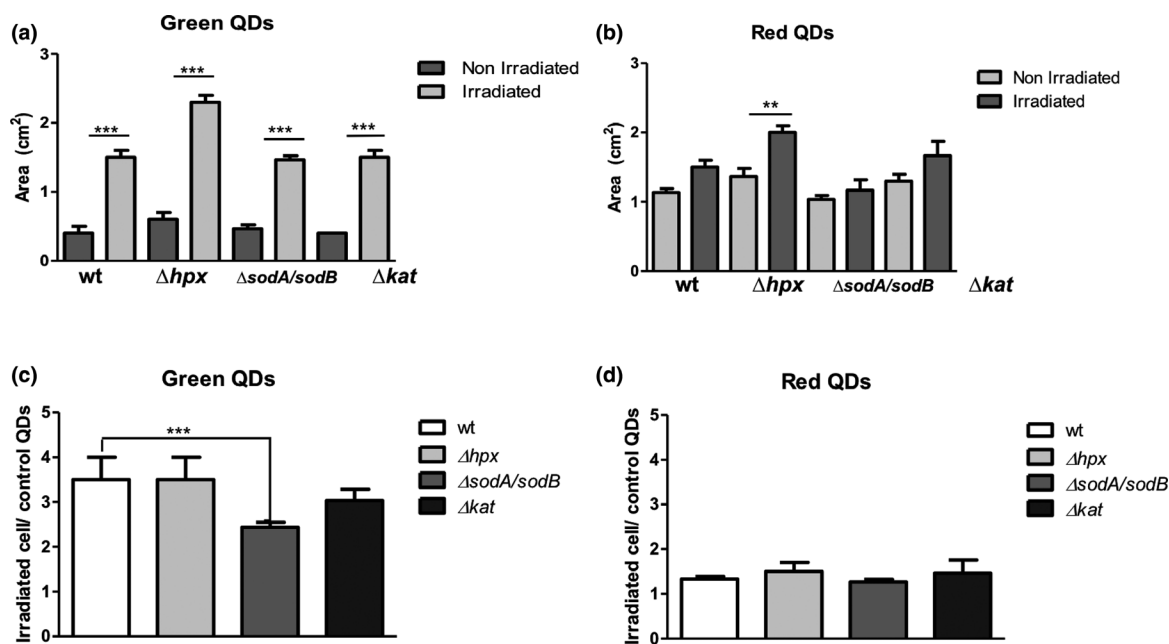


**Figure 5** Phototoxic effect of CdTe-GSH QDs on *Escherichia coli* mutants in ROS defense genes irradiated (5 min) and exposed to (a) green QDs500 or (b) red QDs600. (c) Normalized phototoxic effect (irradiated/non irradiated cells) of (c) green QDs500 and (d) red QDs600. Statistical analysis T-test show \*\*\* $P \leq 0.001$ , \*\* $P \leq 0.01$  and \* $P \leq 0.05$ .

inhibition area when compared to non-irradiated (Fig. 5b). Possibly *hpx* mutant ( $\Delta katG$ ,  $\Delta katE$   $\Delta hpcF$ ) is the most sensible strain because lacks three enzymes that participate in hydrogen peroxide scavenging (Park et al. 2005).

When the growth inhibition effect of QDs in irradiated cells was directly compared with the effect of non-irradiated cells (normalized), green QDs<sub>500</sub> showed the highest phototoxicity in all strains analysed (Fig. 5c,d). In average, a threefold increase in *E. coli* toxicity was observed in cells exposed to irradiated green QDs<sub>500</sub> compared to cells exposed to irradiated red QDs<sub>600</sub>. Obtained results indicate that the phototoxic effect of irradiated cells exposed to green QDs<sub>500</sub> is most probably a consequence of ROS generation.

#### Phototoxic effect of CdTe-GSH QDs on *E. coli* strains deficient in Cd<sup>2+</sup> genes

Since irradiation of green QDs<sub>500</sub> increases the release of cadmium from NPs (Fig. 4), and with the aim of determining the importance of Cd<sup>2+</sup> in QDs phototoxicity, we determined the phototoxic effect of QDs on *E. coli* strains deficient or overexpressing genes involved in Cd<sup>2+</sup> homeostasis (Fig. 6). We studied four strains, two null mutants in *mntH* or *zntA* genes, and two

*E. coli* strains overexpressing *mntH* or *zntA* genes. *mntH* codes for a selective divalent metal ion transporter defined like a proton-dependent manganese transporter that has been related to Cd<sup>2+</sup> uptake (Rensing et al. 1997). *zntA* codes for a Zn (II)/Cd(II)/Pb(II)-translocating P-type ATPase that mediates the efflux of Cd<sup>2+</sup> from cells (Rensing et al. 1997). As reported before, cells lacking the *zntA* gene and those overexpressing *mntH* display increased sensitivity to Cd<sup>2+</sup> (Monrás et al. 2014).

As expected, the *zntA* mutant and the *mntH* overexpressing strains presented increased sensitivity to both QDs when compared to wt *E. coli*. This result confirms the importance of Cd<sup>2+</sup> on QDs toxicity as has been reported before (Monrás et al. 2014). However, when the phototoxic effect of QDs was evaluated, no significant irradiation-dependent increase in bacterial inhibition was determined in most recombinant strains (Fig. 6c,d). The highest phototoxicity of green QDs<sub>500</sub> was evidenced in the wt strain. This result suggests that the phototoxic effect of biomimetic QDs is not mainly related to Cd<sup>2+</sup> release and reinforces the idea that green QDs<sub>500</sub> phototoxicity is mostly associated with ROS generation produced by the release of electrons from photoexcited QDs, reinforcing their potential as PSs in aPDT.

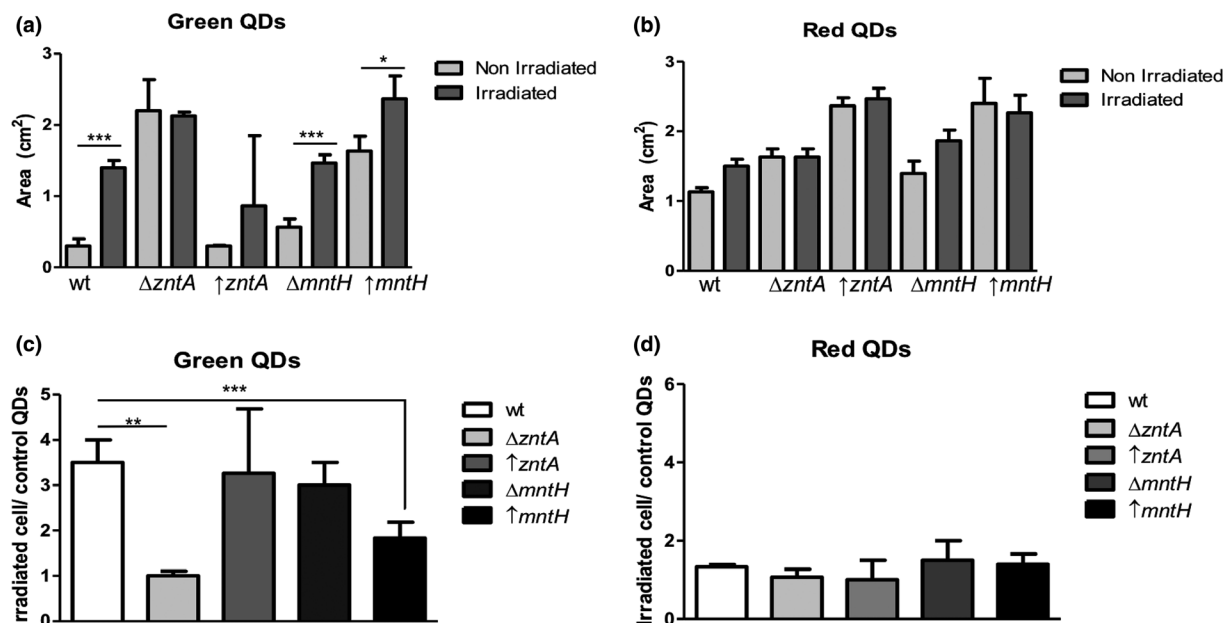


**Figure 6** Phototoxic effect of CdTe-GSH QDs on *Escherichia coli* mutants in cadmium defense genes. Growth inhibition area of *E. coli* strains deficient in Cd<sup>2+</sup> resistance genes exposed to green QDs<sub>500</sub> (a) or red QDs<sub>600</sub> (b) in presence or absence of 5 min irradiation (405 nm). (c) Normalized Phototoxic effect of (c) green QDs<sub>500</sub> and (d) red QDs<sub>600</sub> on *E. coli* BW strains deficient in Cd<sup>2+</sup> resistance genes. Growth irradiation area of cells irradiated were normalized with the control without irradiation. T-test was used for statistical analysis (\*\*\* $P \leq 0.001$ , \*\* $P \leq 0.01$  and \* $P \leq 0.05$ ).



## DISCUSSION

In the present work, we studied the phototoxic mechanism of green and red CdTe-GSH QDs synthesized by a biomimetic method previously reported by our group (Díaz *et al.* 2012; Pérez-Donoso *et al.* 2012; Gautier *et al.* 2013; Molina-Quiroz *et al.* 2013; Monrás *et al.* 2014; Díaz-García *et al.* 2018). Our aim was to evaluate their potential application as PSs in aPDT, a novel antimicrobial therapy that avoids the development of antibiotic bacterial resistance (Almeida *et al.* 2004; Pérez *et al.* 2006; Courtney *et al.* 2016; Kashef *et al.* 2017).

To date, NPs are used in this type of therapy mainly as delivery vehicles for PSs (Ghorbani *et al.* 2018). For example gold nanoparticles (AuNPs) are used as drug-delivery platforms (Chen *et al.* 2016) and also as surface plasmon-enhanced agents (Chu *et al.* 2016; Kashef *et al.* 2017). On the other hand, Misba *et al.* determined a significant effect on *Streptococcus mutans* biofilms by conjugating toluidine blue O with AgNP (Misba *et al.* 2016; Kashef *et al.* 2017). Nevertheless, NPs themselves can act as PS because they are able to absorb light in specific regions of the electromagnetic spectrum, allowing the transition of electrons to excited states that can lead to photochemical generation of ROS. Examples of these NPs include fullerenes, TiO<sub>2</sub>, QDs, even up conversion nanoparticles (UCNPs) (Kashef *et al.* 2017), molybdenum oxide, ZnO and tungsten oxide (Sun *et al.* 2018). After light exposure, TiO<sub>2</sub> NPs mediate the photo-oxidation of oxygen to produce ROS. Lipovsky *et al.* (2011) examined the bactericidal properties after exposure to visible light of a mixture of TiO<sub>2</sub> and ZnO NPs, and determined ~80–90% reduction in viability of *S. aureus* and *Staphylococcus epidermidis*.

The excellent properties of QDs as PS have been extensively reported and are mostly associated with their small diameter (2–4 nm) that allows their movement through cellular membranes, accumulation in the intracellular environment and generation of specific light-activated redox species (Lu *et al.* 2008; Courtney *et al.* 2016). Courtney *et al.* (2016) showed that after 6 h treatment with CdTe-2.4 and illumination, the number of viable *E. coli* cells decreased (80% of cells killed). So, they probed that in presence of 100 nmol l<sup>-1</sup> CdTe-2.4 and light, the growth of *S. aureus* was reduced 29%, *K. pneumoniae* 59% and *SalmonellaTyphimurium* 56%. These NPs were synthesized through a chemical method that requires high temperatures to produce QDs of different sizes. Using QDs as PS is a significant contribution to aPDT, however, the expensive methods required for NPs synthesis and their basal toxicity have limited their use.

Biomimetic CdTe-GSH QDs (patent no. US 20130284979) are synthesized using a simple and low-cost

procedure (Díaz *et al.* 2012; Pérez-Donoso *et al.* 2012). These NPs have a wide absorption of light, emission and photostability (Díaz *et al.* 2012; Pérez-Donoso *et al.* 2012; Gautier *et al.* 2013; Monrás *et al.* 2014; Díaz-García *et al.* 2018). We have previously studied its toxic effect on *E. coli*, *B. subtilis*, *K. pneumoniae* and *S. aureus* (Díaz *et al.* 2012), determining that CdTe-GSH QDs generate oxidative stress in cells as a consequence of the release of Cd<sup>2+</sup> ions from the nanocrystal, being red QDs<sub>600</sub> the most toxic for bacterial cells (Díaz *et al.* 2012; Pérez-Donoso *et al.* 2012; Gautier *et al.* 2013; Monrás *et al.* 2014; Díaz-García *et al.* 2018). In addition, we also studied their effect on biological systems *in vivo*, validating their biocompatibility and confirming that biomimetic QDs-GSH represent a potential alternative for medical treatments (Díaz-García *et al.* 2018).

In the present work, we evaluated the phototoxic effect of green and red biomimetic QDs in *E. coli*. In agreement with the reported biocompatibility of biomimetic QDs, no significant effect on viability was determined when *E. coli* cells were exposed to 400 µg ml<sup>-1</sup> of green or red QDs-GSH (Fig. 2a,b). In contrast, a significant decrease in cell viability was observed in cells exposed to photoactivated QDs. A significant decrease in viability was observed after 5- and 10 min-exposure to irradiated green and red QDs, respectively (Fig. 2e). Viability differences between irradiated cells exposed to green and red QDs could be associated with the higher reduction power of green QDs<sub>500</sub> that could favour ROS generation (Nozik 1978; Katari *et al.* 1994). The ability to adjust the electronic properties of semiconductor nanomaterials provides a way to induce specific disturbances in redox environments by altering the electronic state of QDs, whose alteration will depend on their size, shape or composition. In addition, the excitation of QDs with light emission above its nominal bandgap can allow the generation of ROS (Sun *et al.* 2014; Courtney *et al.* 2016).

The generation of ROS in cells exposed to photoactivated green QDs<sub>500</sub> occurs at early irradiation times (5 min), similar to that observed in the positive control H<sub>2</sub>O<sub>2</sub> (Fig. 3). This could be a consequence of the entry of irradiated QDs inside cells causing a higher toxic effect mediated by the release of electrons that in presence of oxygen could generate superoxide ions and cause oxidative stress (see proposed model of Fig. 7e). On the other hand, when irradiated cells are exposed to red QDs, the toxic effect is minor than that produced by green irradiated QDs, and the difference in ROS generation between irradiated and non-irradiated cells exposed to red QDs is only significant after 20 min irradiation. This result suggests that the toxic effect of red QDs in cells is mostly associated with the release of Cd<sup>2+</sup> ions from the nanocrystal, and not with the local release of electrons

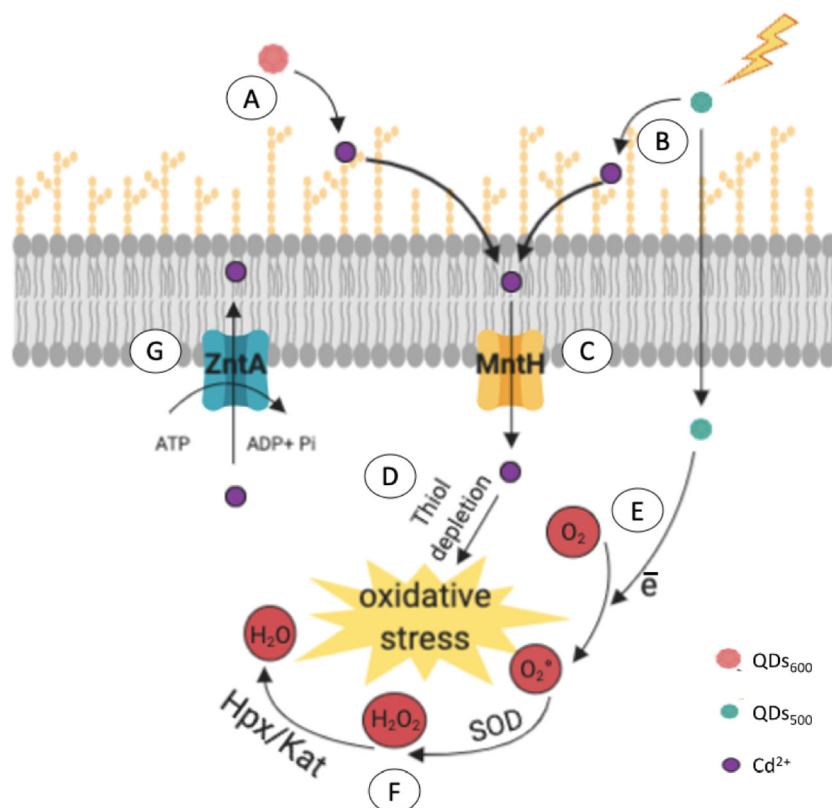


**Figure 7** Model explaining the phototoxic effect of biomimetic CdTe-GSH QDs in *Escherichia coli*. (a) Cd<sup>2+</sup> ions released from red CdTe-GSH NPs in absence of irradiation. (b) Cd<sup>2+</sup> ions released from green CdTe-GSH NPs after irradiation. (c) Cell uptake of Cd<sup>2+</sup> ions through the MntH transporter. (d) Cd<sup>2+</sup> ions generate thiol depletion and oxidative stress in *E. coli* cells. (e) Irradiation of green CdTe-GSH NPs favors the generation of ROS inside cells through electron-transfer reactions. (f) Cellular response to oxidative stress mediated by SOD and Hpx/Kat enzymes. (g) The P-Type ATPase ZntA participates in the cellular response to QDs through the efflux of Cd<sup>2+</sup> ions released from the nanocrystal (mainly red QDs).

that can directly generate ROS, as in the case of irradiated green QDs<sub>500</sub> (Fig. 7b).

PS react in the presence of molecular oxygen to produce two types of photochemical reactions, Type I or Type II (Almeida *et al.* 2004). Type I photo processes involve hydrogen or electron-transfer reactions between the excited state PS and other molecules in the environment. These electron-transfer reactions generate ROS that are harmful to cells. Type II photo process is an energy-transfer mechanism involving electron spin exchange between the excited triplet state PS and ground state oxygen (3O<sub>2</sub>). Both reactions produce ROS that can cause the oxidation of biomolecules (lipids, proteins and nucleic acids) in cells (Kashef *et al.* 2017).

Irradiated green QDs present a lower release of Cd<sup>2+</sup> ions when compared with irradiated red QDs (Fig. 4). In non-irradiated green QDs, the release of Cd ions is half of all other conditions, similar to what was previously

observed (Ochi *et al.* 1988; Derfus *et al.* 2004; Hardman 2006; Rzigalinski and Strobl 2009; Monrás *et al.* 2014). The release of Cd<sup>2+</sup> ions from red QDs is high, which can indirectly generate ROS at longer times as a consequence of metal-mediated reactions and thiol depletion (Fig. 7d). At the cellular level, cadmium induces damage and repair mechanisms in which the cellular redox state plays a crucial role. Since it is not redox-active, Cd<sup>2+</sup> cannot directly generate ROS, but oxidative stress induced by Cd<sup>2+</sup> is a common phenomenon observed in multiple studies (Cuypers *et al.* 2010). Also, it has been reported that once inside the cell, due to its affinity with thiol groups, Cd<sup>2+</sup> causes a depletion of thiol groups that conducts to oxidative stress (Wang *et al.* 2004). However, observed ROS production is not directly related to metal release since in the absence of irradiation (when high levels of cadmium are released) no significant increase in ROS levels and cell death were observed.

To understand this phenomenon, we analysed the phototoxicity of red and green QDs in *E. coli* strains lacking genes involved in ROS and Cd-response. *Escherichia coli* mutants in genes related to ROS response were more sensitive than the wt strains to the phototoxic effect of green QDs<sub>500</sub>, which reinforce the idea that the phototoxic effect of green QDs<sub>500</sub> involves ROS generation (Fig. 7b). On the other hand, no increase in the phototoxic effect of green irradiated QDs<sub>500</sub> was observed in *E. coli* mutants deficient in Cd<sup>2+</sup> response genes ( $\Delta zntA$  or over-expressing *mntH*), confirming that the observed effect of green QD<sub>500</sub> is not related to Cd<sup>2+</sup> release from the nanocrystal (Fig. 7).

Thus, the higher reduction potential of green QDs added to their smaller size (3 nm) improves their efficiency to kill cells after irradiation. Photoinduced toxicity is a consequence of their capacity to transfer electrons and produce ROS, increasing the oxidative stress inside cells (Fig. 7). On the other hand, red QDs mostly affect cells as a consequence of the oxidative damage indirectly generated by Cd<sup>2+</sup> release from the NP core, in a process that is independent of light irradiation.

Altogether, obtained results indicate that green QDs<sub>500</sub> are good candidates for PDT in antimicrobials since their toxicity can be induced by irradiation. These promising results invite us to develop new technologies for the specific delivery of QDs. The surface of biomimetic CdTe-GSH QDs can be fused with cations, molecules, aptamers or antibodies to facilitate their delivery to target cells or tissues. In addition, another advantage of using QDs in aPDT is its spectral properties that can be adjusted to improve spectral overlap with organic PSs, improving fluorescence resonance energy transfer and aPDT efficiency.

## Acknowledgements

This work was supported by Erika Elcira Donoso Lopez. The authors also thank Ms. Yuly Straub for their contribution to the experiments and discussion of this work. In the loving memory of Claudio Vásquez Guzmán, an excellent friend, mentor and scientist, but a better human being. Thanks for all the adventures, and for showing us the beauty of science and friendship. As you always said Que nos deparará el futuro?

## Author contributions

JP-D conceived and designed the study. NO, CM and JP-D performed the experiments and analysed data. NO, DB, CV and JP-D wrote the paper. All authors contributed to the scientific discussion and revision of the manuscript.

## Funding

Fondecyt 1200870 (JP-D, DB), Fondecyt 3190555 (NO) and INACH RT-25\_16 (JP-D, DB) supported this work.

## Conflict of Interest

The authors have no conflict of interest.

## REFERENCES

- Abramson, A.L., Shikowitz, M.J., Mullyooly, V.M., Steinberg, B.M., Amella, C.A. and Rothstein, H.R. (1992) Clinical effects of photodynamic therapy on recurrent laryngeal papillomas. *Arch Otolaryngol-Head Neck Surg* **118**, 25–29. <https://doi.org/10.1001/archotol.1992.01880010029011>
- Åkerman, M.E., Chan, W.C.W., Laakkonen, P., Bhatia, S.N. and Ruoslahti, E. (2002) Nanocrystal targeting in vivo. *Proc Natl Acad Sci* **99**, 12617–12621. [10.1073/pnas.152463399](https://doi.org/10.1073/pnas.152463399).
- Aldana, J., Wang, Y.A., and Peng X. (2001). Photochemical instability of CdSe nanocrystals coated by hydrophilic thiols. *J Am Chem Soc.* **123**, 8844–8850. <https://doi.org/10.1021/ja016424q>
- Almeida, R.D., Manadas, B.J., Carvalho, A.P. and Duarte, C.B. (2004) Intracellular signaling mechanisms in photodynamic therapy. *Biochim Biophys Acta Rev Cancer* **1704**, 59–86. <https://doi.org/10.1016/j.bbcan.2004.05.003>
- Asilian, A. and Davami, M. (2006) Comparison between the efficacy of photodynamic therapy and topical paromomycin in the treatment of Old World cutaneous leishmaniasis: a placebo-controlled, randomized clinical trial. *Clin Exp Dermatol* **31**, 634–637. <https://doi.org/10.1111/j.1365-2230.2006.02182.x>
- Baba, T., Ara, T., Hasegawa, M., Takai, Y., Okumura, Y., Baba, M., Datsenko, K.A., Tomita, M. et al. (2006) Construction of *Escherichia coli* K-12 in-frame, single-gene knockout mutants: The Keio collection. *Molecular Systems Biology* **2**, <https://doi.org/10.1038/msb4100050>
- Celli, J.P., Spring, B.Q., Rizvi, I., Evans, C.L., Samkoe, K.S., Verma, S., Pogue, B.W. and Hasan, T. (2010) Imaging and photodynamic therapy: Mechanisms, monitoring, and Optimization. *Chem Rev* **110**, 2795–2838. <https://doi.org/10.1021/cr900300p>
- Chen, C., Peng, J., Sun, S.-R., Peng, C.-W., Li, Y. and Pang, D.-W. (2012) Tapping the potential of quantum dots for personalized oncology: current status and future perspectives. *Nanomedicine* **7**, 411–428. <https://doi.org/10.2217/nmm.12.9>
- Chen, R.J., Chen, P.-C., Prasannan, A., Vinayagam, J., Huang, C.-C., Chou, P.-Y., Weng, C.-C., Tsai, H.C. et al. (2016) Formation of gold decorated porphyrin nanoparticles and evaluation of their photothermal and photodynamic

- activity. *Mat Sci Eng C* **63**, 678–685. <https://doi.org/10.1016/j.msec.2016.03.034>
- Christodoulides, N., Nikolidakis, D., Chondros, P., Becker, J., Schwarz, F., Rössler, R. and Sculean, A. (2008) Photodynamic therapy as an adjunct to non-surgical periodontal treatment: a randomized, controlled clinical trial. *J Periodontol* **79**, 1638–1644. <https://doi.org/10.1902/jop.2008.070652>
- Chu, C.K., Tu, Y.-C., Hsiao, J.-H., Yu, J.-H., Yu, C.-K., Chen, S.-Y., Tseng, P.-H., Chen, S. et al. (2016) Combination of photothermal and photodynamic inactivation of cancer cells through surface plasmon resonance of a gold nanoring. *Nanotechnology* **27**. <https://doi.org/10.1088/0957-4484/27/11/115102>
- Cieplik, F., Deng, D., Crielaard, W., Buchalla, W., Hellwig, E., Al-Ahmad, A. and Maisch, T. (2018) Antimicrobial photodynamic therapy—what we know and what we don't. *Crit Rev Microbiol* **44**, 571–589. doi:10.1080/1040841X.2018.1467876
- Courtney, C.M., Goodman, S.M., McDaniel, J.A., Madinger, N.E., Chatterjee, A. and Nagpal, P. (2016) Photoexcited quantum dots for killing multidrug-resistant bacteria. *Nat Mater* **15**, 529–534. <https://doi.org/10.1038/nmat4542>
- Cuyppers, A., Plusquin, M., Remans, T., Jozefczak, M., Keunen, E., Gielen, H., Opdenakker, K., and Nair, A.R. (2010) Cadmium stress: an oxidative challenge. *Biometals* **23**, 927–940. <https://doi.org/10.1007/s10534-010-9329-x>
- da Mota, A.C.C., Gonçalves, M.L.L., Bortoletto, C., Olivian, S.R., Salgueiro, M., Godoy, C., Altavista, O.M., Pinto, M.M. et al. (2015) Evaluation of the effectiveness of photodynamic therapy for the endodontic treatment of primary teeth: study protocol for a randomized controlled clinical trial. *Trials* **16**, 2–7. <https://doi.org/10.1186/s13063-015-1086-2>
- Datsenko, K.A. and Wanner, B.L. (2000) One-step inactivation of chromosomal genes in *Escherichia coli* K-12 using PCR products. *Proc Nat Acad Sci USA*, **97**, 6640–6645. 10.1073/pnas.120163297.
- Delehanty, J.B., Boeneman, K., Bradburne, C.E., Robertson, K. and Medintz, I.L. (2009) Quantum dots: a powerful tool for understanding the intricacies of nanoparticle-mediated drug delivery. *Expert Opin Drug Del* **6**, 1091–1112. <https://doi.org/10.1517/17425240903167934>
- Derfus, A.M., Chan, W.C.W. and Bhatia, S.N. (2004) Probing the cytotoxicity of semiconductor quantum dots. *Nano Lett* **4**, 11–18. <https://doi.org/10.1021/nl0347334>
- Dharmaraja, A.T. (2017) Role of reactive oxygen species (ROS) in therapeutics and drug resistance in cancer and bacteria. *J Med Chem* **60**, 3221–3240. <https://doi.org/10.1021/acs.jmedchem.6b01243>
- Díaz-García, V.M., Guerrero, S., Díaz-Valdivia, N., Lobos-González, L., Kogan, M., Pérez-Donoso, J.M. & Quest, A.F. (2018) Biomimetic quantum dot-labeled B16F10 murine melanoma cells as a tool to monitor early steps of lung metastasis by in vivo imaging. *Int J Nanomed* **13**, 6391–6412. <https://doi.org/10.2147/IJN.S165565>
- Díaz, V., Ramírez-Maureira, M., Monrás, J.P., Vargas, J., Bravo, D., Osorio-Román, I.O., Vásquez, C.C. and Pérez-Donoso, J.M. (2012) Spectroscopic properties and biocompatibility studies of CdTe quantum dots capped with biological thiols. *Sci Adv Mat* **4**, 609–616. <https://doi.org/10.1166/sam.2012.1327>
- Ferreira, J., Kurachi, C., Moriyama, L.T., Menezes, P.F.C., Perussi, J.R., Sibata, C., Zucoloto, S., Castro e Silva Jr, O. et al. (2006) Correlation between the photostability and photodynamic efficacy for different photosensitizers. *Laser Phys Lett* **3**, 91–95. <https://doi.org/10.1002/lapl.200510057>
- Ferreira, J., Menezes, P.F.C., Kurachi, C., Sibata, C.H., Allison, R.R. and Bagnato, V.S. (2007) Comparative study of photodegradation of three hematoporphyrin derivative: Photofrin®, Photogem®, and Photosan®. *Laser Phys Lett* **4**, 743–748. <https://doi.org/10.1002/lapl.200710058>
- Gaponik, N., Talapin, D.V., Rogach, A.L., Hoppe, K., Shevchenko, E.V., Kornowski, A., Eychmüller, A. & Weller, H. (2002) Thiol-Capping of CdTe Nanocrystals: An Alternative to Organometallic Synthetic Routes. *The Journal of Physical Chemistry B*, **106**(29), 7177–7185. <https://doi.org/10.1021/jp025541k>
- Gautier, J.L., Monrás, J.P., Osorio-Román, I.O., Vásquez, C.C., Bravo, D., Herranz, T., Marco, J.F. and Pérez-Donoso, J.M. (2013) Surface characterization of GSH-CdTe quantum dots. *Mat Chem Phys* **140**, 113–118. <https://doi.org/10.1016/j.matchemphys.2013.03.008>
- Ghorbani, J. et al. (2018) Photosensitizers in antibacterial photodynamic therapy: an overview. *Laser Therapy* **27**, 293–302. [https://doi.org/10.5978/islsm.27\\_18-RA-01](https://doi.org/10.5978/islsm.27_18-RA-01)
- Grill, E., Winnacker, E.-I. and Zenk, M.H. (1985) Phytochelatins: the principal heavy-metal complexing peptides of higher plants. *Science* **230**, 674–676. <https://doi.org/10.1126/science.230.4726.674>
- Hardman, R. (2006) A toxicologic review of quantum dots: toxicity depends on physicochemical and environmental factors. *Environ Health Perspect* **114**, 165–172. <https://doi.org/10.1289/ehp.8284>
- Helbig, K., Bleuel, C., Krauss, G.J. and Nies, D.H. (2008) Glutathione and transition-metal homeostasis in *Escherichia coli*. *J Bacteriol* **190**, 5431–5438. <https://doi.org/10.1128/JB.00271-08>
- Henderson, B.W. and Dougherty, T.J. (1992) How does photodynamic therapy work? *Photochem Photobiol* **55**, 145–157. <https://doi.org/10.1111/j.1751-1097.1992.tb04222.x>
- Yi, G., Hong, S.H., Son, J., Yoo, J., Park, C., Choi, Y. and Koo, H. (2018) Recent advances in nanoparticle carriers for photodynamic therapy. *Quant Imag Med Surg* **8**, 433–443. <https://doi.org/10.21037/qims.2018.05.04>
- Iravani, S., Korbekandi, H., Mirmohammadi, S.V. and Zolfaghari, B. (2016) Synthesis of silver nanoparticles: chemical, physical and biological methods. Synthesis of

- silver NPs. *Res Pharm Sci* **9**, 1–17. <https://doi.org/10.1111/j.1551-2916.2006.01044.x>
- Kashef, N., Huang, Y.-Y. and Hamblin, M.R. (2017) Advances in antimicrobial photodynamic inactivation at the nanoscale. *Nanophotonics* **6**, 853–879. <https://doi.org/10.1515/nanoph-2016-0189>
- Katari, J.E.B., Colvin, V.L. and Alivisatos, A.P. (1994) X-ray photoelectron spectroscopy of CdSe nanocrystals with applications to studies of the nanocrystal surface. *J Phys Chem* **98**, 4109–4117. <https://doi.org/10.1021/j100066a034>
- Kharkwal, G.B., Sharma, S.K., Huang, Y.-Y., Dai, T. and Hamblin, M.R. (2011) Photodynamic therapy for infections: clinical applications. *Laser Surg Med* **43**, 755–767. <https://doi.org/10.1002/lsm.21080>
- Koshi, E., Mohan, A., Rajesh, S. and Philip, K. (2011) Antimicrobial photodynamic therapy: an overview. *Journal of Indian Society of Periodontology* **15**, 323. <https://doi.org/10.4103/0972-124X.92563>
- Lewinski, N., Colvin, V. and Drezek, R. (2008) Cytotoxicity of nanoparticles. In ed. Faisal, M. et al. *Small*. vol. **4**, pp. 26–49. Cham: Springer International Publishing. <https://doi.org/10.1002/smll.200700595>
- Li, K.G., Chen, J.T., Bai, S.S., Wen, X., Song, S.Y., Yu, Q., Li, J. and Wang, Y.Q. (2009) Intracellular oxidative stress and cadmium ions release induce cytotoxicity of unmodified cadmium sulfide quantum dots. *Toxicol In Vitro* **23**, 1007–1013. <https://doi.org/10.1016/j.tiv.2009.06.020>
- Lipovsky, A., Gedanken, A., Nitzan, Y. and Lubart, R. (2011) Enhanced inactivation of bacteria by metal-oxide nanoparticles combined with visible light irradiation. *Lasers Surg Med* **43**, 236–240. <https://doi.org/10.1002/lsm.21033>
- Lombard, G.F.S.T. and Lanotte, M.M. (ed.) (1985) *The Treatment of Neurosurgical Infections by Lasers and Porphyrins*. Padova: Edizione Libreria Progetto, pp. 363–366.
- Lovrić, J. et al. (2005) Differences in subcellular distribution and toxicity of green and red emitting CdTe quantum dots. *J Mol Med* **83**, 377–385. <https://doi.org/10.1007/s00109-004-0629-x>
- Lu, Z., Li, C.M., Bao, H., Qiao, Y., Toh, Y. and Yang, X. (2008) Mechanism of antimicrobial activity of CdTe quantum dots. *Langmuir* **24**, 5445–5452. <https://doi.org/10.1021/la704075r>
- Michailov, N., Peeva, M., Angelov, I., Wohrle, D., Muller, S., Jori, G., Ricchelli, F. and Shopova, M. (1997) Fluence rate effects on photodynamic therapy of B16 pigmented melanoma. *J Photochem Photobiol B* **37**, 154–157. [https://doi.org/10.1016/S1011-1344\(96\)07401-5](https://doi.org/10.1016/S1011-1344(96)07401-5)
- Misba, L. et al. (2016) Antibiofilm action of a toluidine blue O-silver nanoparticle conjugate on *Streptococcus mutans*: a mechanism of type I photodynamic therapy. *Biofouling* **32**, 313–328. <https://doi.org/10.1080/08927014.2016.1141899>
- Molina-Quiroz, R.C. et al. (2013) DNA, cell wall and general oxidative damage underlie the tellurite/cefotaxime synergistic effect in *Escherichia coli*. *PLoS One* **8**, <https://doi.org/10.1371/journal.pone.0079499>
- Molina-Quiroz, R.C., Loyola, D.E., Díaz-Vásquez, W.A., Arenas, F.A., Urzúa, U., Pérez-Donoso, J.M. and Vásquez, C.C. (2014) Global transcriptomic analysis uncovers a switch to anaerobic metabolism in tellurite-exposed *Escherichia coli*. *Res Microbiol* **165**, 566–570. <https://doi.org/10.1016/j.resmic.2014.07.003>
- Monrás, J.P., Díaz, V., Bravo, D., Montes, R.A., Chasteen, T.G., Osorio-Román, I.O., Vásquez, C.C. & Pérez-Donoso, J.M. (2012) Enhanced glutathione content allows the in vivo synthesis of fluorescent CdTe nanoparticles by *Escherichia coli*. *PLoS One*, **7**(11), e48657.
- Monrás, J.P., Monrás, J.P., Collao, B., Molina-Quiroz, R.C., Pradenas, G.A., Saona, L.A., Durán-Toro, V., Órdenes-Aenishanslins, N. et al. (2014) Microarray analysis of the *Escherichia coli* response to CdTe-GSH quantum dots: understanding the bacterial toxicity of semiconductor nanoparticles. *BMC Genom* **15**, 1099. <https://doi.org/10.1186/1471-2164-15-1099>
- Nishiyama, N., Morimoto, Y., Jang, W.-D. and Kataoka, K. (2009) Design and development of dendrimer photosensitizer-incorporated polymeric micelles for enhanced photodynamic therapy. *Adv Drug Deliv Rev* **61**, 327–338. <https://doi.org/10.1016/j.addr.2009.01.004>
- Nozik, A.J. (1978) ‘Photoelectrochemistry: applications to Solar Energy Conversion’. *Ann Rev Phys Chem* **29**, 189–222. <https://doi.org/10.1146/annurev.pc.29.100178.001201>
- Ochi, T., Otsuka, F., Takahashi, K. and Ohsawa, M. (1988) Glutathione and metallothioneins as cellular defense against cadmium toxicity in cultured Chinese hamster cells. *Chem Biol Interact* **65**, 1–14. [https://doi.org/10.1016/0009-2797\(88\)90026-9](https://doi.org/10.1016/0009-2797(88)90026-9)
- de Oliveira, B.P., Aguiar, C.M. and Câmara, A.C. (2014) Photodynamic therapy in combating the causative microorganisms from endodontic infections. *Eur J Dentist* **8**, 424–430. <https://doi.org/10.4103/1305-7456.137662>
- Park, S., You, X. and Imlay, J.A. (2005) Substantial DNA damage from submicromolar intracellular hydrogen peroxide detected in Hpx-mutants of *Escherichia coli*. *Proc Natl Acad Sci USA* **102**, 9317–9322. <https://doi.org/10.1073/pnas.0502051102>
- Pérez-Donoso, J.M., Monrás, J.P., Bravo, D., Aguirre, A., Quest, A.F., Osorio-Román, I.O., Aroca, R.F., Chasteen, T.G. et al. (2012) Biomimetic, mild chemical synthesis of CdTe-GSH quantum dots with improved biocompatibility. *PLoS One* **7**, e30741. <https://doi.org/10.1371/journal.pone.0030741>
- Pérez, J.M. et al. (2006) *Geobacillus stearothermophilus* LV cadA gene mediates resistance to cadmium, lead and zinc in zntA mutants of *Salmonella serovar typhimurium*. *Biol Res* **39**, 661–668. <https://doi.org/10.4067/s0716-97602006000500009>
- Pérez, J.M., Calderón, I.L., Arenas, F.A., Fuentes, D.E., Pradenas, G.A., Fuentes, E.L., Sandoval, J.M., Castro, M.E.

- et al. (2007) Bacterial toxicity of potassium tellurite: Unveiling an ancient enigma. *PLoS One* **2**, e211. doi: 10.1371/journal.pone.0000211.
- Pons, T. et al. (2010) Cadmium-free CuInS<sub>2</sub>/ZnS quantum dots for sentinel lymph node imaging with reduced toxicity. *ACS Nano* **4**, 2531–2538. <https://doi.org/10.1021/nn901421v>
- Qu, Y. and Lü, X. (2009) Aqueous synthesis of gold nanoparticles and their cytotoxicity in human dermal fibroblasts–fetal. *Biomed Mater* **4**, 025007. <https://doi.org/10.1088/1748-6041/4/2/025007>
- Rensing, C. et al. (1997) The zntA gene of *Escherichia coli* encodes a Zn(II)-translocating P-type ATPase (zinc transport/zinc resistance/cadmium resistance). *Biochemistry* **94**, 14326–14331.
- Renwick, M.J., Simpkin, V. and Mossialos, E. (2016) E. Targeting innovation in antibiotic drug discovery and development: the need for a One Health – one Europe – one World Framework. Copenhagen, Denmark.
- Rzagalinski, B.A. and Strobl, J.S. (2009) Cadmium-containing nanoparticles: perspectives on pharmacology and toxicology of quantum dots. *Toxicol Appl Pharmacol* **238**, 280–288. doi:10.1016/j.taap.2009.04.010.
- SB B.Clinical developments in antimicrobial PDT. 12th International Photodynamic Association World Congress 2009, Seattle.
- Schafer, F.Q. and Buettner, G.R. (2001) Redox environment of the cell as viewed through the redox state of the glutathione disulfide/glutathione couple. *Free Radic Biol Med* **30**, 1191–1212. [https://doi.org/10.1016/S0891-5849\(01\)00480-4](https://doi.org/10.1016/S0891-5849(01)00480-4)
- Rosenblum, L.T. et al. (2010) In vivo molecular imaging using nanomaterials: general in vivo characteristics of nano-sized reagents and applications for cancer diagnosis (Review). *Mol Membr Biol* **27**, 274–285. <https://doi.org/10.3109/09687688.2010.481640>
- Shikowitz, M.J., Abramson, A.L., Freeman, K., Steinberg, B.M. and Nouri, M. (1998) Efficacy of DHE photodynamic therapy for respiratory papillomatosis: immediate and long-term results. *Laryngoscope* **108**, 962–967. <https://doi.org/10.1097/00005537-199807000-00002>
- Smith, A.M., Duan, H., Mohs, A. and Nie, S. (2008) Bioconjugated quantum dots for in vivo molecular and cellular imaging. *Adv Drug Deliv Rev* **60**, 1226–1240. <https://doi.org/10.1016/j.addr.2008.03.015>
- Song, J., Kang, H., Lee, C., Hwang, S.H. and Jang, J. (2012) Aqueous synthesis of silver nanoparticle embedded cationic polymer nanofibers and their antibacterial activity. *ACS Appl Mater Interfaces* **4**, 460–465. <https://doi.org/10.1021/am201563t>
- Souza, L.C., Brito, P.R.R., Machado de Oliveira, J.C., Alves, F.R.F., Moreira, E.J.L., Sampaio-Filho, H.R., Rôças, I.N. and Siqueira Jr, J.F. (2010) Photodynamic therapy with two different photosensitizers as a supplement to instrumentation/irrigation procedures in promoting intracanal reduction of *Enterococcus faecalis*. *J Endodontic* **36**, 292–296. <https://doi.org/10.1016/j.joen.2009.09.041>
- Sun, J., Kormakov, S., Liu, Y., Huang, Y., Wu, D. and Yang, Z. (2018) Recent progress in metal-based nanoparticles mediated photodynamic therapy. *Molecules* **23**, 1704. <https://doi.org/10.3390/molecules23071704>
- Sun, Q.C., Mundoor, H., Ribot, J.C., Singh, V., Smalyukh, I.I. and Nagpal, P. (2014) Plasmon-enhanced energy transfer for improved upconversion of infrared radiation in doped-lanthanide nanocrystals. *Nano Lett* **14**, 101–106. <https://doi.org/10.1021/nl403383w>
- Venegas, F.A., Saona, L.A., Monrás, J.P., Órdenes-Aenishanslins, N., Giordana, M.F., Ulloa, G., Colloa, B., Bravo, D. et al. (2017) Biological phosphorylated molecules participate in the biomimetic and biological synthesis of cadmium sulphide quantum dots by promoting H<sub>2</sub>S release from cellular thiols. *RSC Advances*, **7**(64), 40270–40278.
- Wang, C.W., Ding, H.-P., Xin, G.-Q., Chen, X., Lee, Y. Ill, Hao, J. and Liu, H.-G. (2009) Silver nanoplates formed at the air/water and solid/water interfaces. *Colloids Surf A* **340**, 93–98. <https://doi.org/10.1016/j.colsurfa.2009.03.003>
- Wang, Y., Fang, J., Leonard, S.S. and Krishna Rao, K.M. (2004) Cadmium inhibits the electron transfer chain and induces reactive oxygen species. *Free Radic Biol Med* **36**, 1434–1443. <https://doi.org/10.1016/j.freeradbiomed.2004.03.010>
- Wolf, P., Rieger, E. and Kerl, H. (1993) Topical photodynamic therapy with endogenous porphyrins after application of 5-aminolevulinic acid. *J Am Acad Dermatol* **28**, 17–21. [10.1016/0190-9622\(93\)70002-B](https://doi.org/10.1016/0190-9622(93)70002-B).
- Ye, S., Yan, M., Tan, X., Liang, J., Zeng, G., Wu, H., Song, B., Zhou, C. et al. (2019) Facile assembled biochar-based nanocomposite with improved graphitization for efficient photocatalytic activity driven by visible light. *Appl Catal B* **250**, 78–88. <https://doi.org/10.1016/j.apcatb.2019.03.004>
- Ye, S., Zeng, G., Tan, X., Wu, H., Liang, J., Song, B., Tang, N., Zhang, P. et al. (2020) Nitrogen-doped biochar fiber with graphitization from *Boehmeria nivea* for promoted peroxymonosulfate activation and non-radical degradation pathways with enhancing electron transfer. *Appl Catal B Environ* **269**, 118850. <https://doi.org/10.1016/j.apcatb.2020.118850>
- You, J., Xiang, M., Hu, H., Cai, J., Zhou, J. and Zhang, Y. (2013) Aqueous synthesis of silver nanoparticles stabilized by cationic cellulose and their catalytic and antibacterial activities. *RSC Adv* **3**, 19319–19329. <https://doi.org/10.1039/c3ra42242a>
- Zheng, Y., Gao, S. and Ying, J.Y. (2007) Synthesis and cell-imaging applications of glutathione-capped CdTe quantum dots. *Adv Mat* **19**, 376–380. <https://doi.org/10.1002/adma.200600342>